Otology & Neurotology
29:846–853 © 2008, Otology & Neurotology, Inc.

The ErbB Inhibitors Trastuzumab and Erlotinib Inhibit Growth of Vestibular Schwannoma Xenografts in Nude Mice: A Preliminary Study

J. Jason Clark, Matthew Provenzano, Henry R. Diggelmann, Ningyong Xu, Skylar S. Hansen, and Marlan R. Hansen

Department of Otolaryngology–Head and Neck Surgery, University of Iowa, Iowa City, Iowa, U.S.A.

Objective: To analyze the ability of ErbB inhibitors to reduce the growth of vestibular schwannoma (VS) xenografts.
Methods: Vestibular schwannoma xenografts were established in the interscapular fat pad in nude mice for 4 weeks. Initially, a small cohort of animals was treated with the ErbB2 inhibitor trastuzumab or saline for 2 weeks. Animals also received bromodeoxyuridine injections to label proliferating cells. In a longer-term experiment, animals were randomized to receive trastuzumab, erlotinib (an ErbB kinase inhibitor), or placebo for 12 weeks. Tumor growth was monitored by magnetic resonance imaging during the treatment period. Cell death was analyzed by terminal deoxynucleotidyl transferase–mediated dUTP-biotin end labeling of fragmented DNA.
Results: Tumors can be distinguished with T2-weighted magnetic resonance imaging sequences. Trastuzumab significantly reduced the proliferation of VS cells compared with control ($p < 0.01$) as analyzed by bromodeoxyuridine uptake. Control tumors demonstrated slight growth during the 12-week treatment period. Both trastuzumab and erlotinib significantly reduced the growth of VS xenografts ($p < 0.05$). Erlotinib, but not trastuzumab, resulted in a significant increase in the percentage of terminal deoxynucleotidyl transferase–mediated dUTP-biotin end labeling of fragmented DNA–positive VS cells ($p < 0.01$).
Conclusion: In this preliminary study, the ErbB inhibitors trastuzumab and erlotinib decreased growth of VS xenografts in nude mice, raising the possibility of using ErbB inhibitors in the management of patients with schwannomas, particularly those with neurofibromatosis Type 2. **Key Words:** Acoustic neuroma—Apoptosis—Cell proliferation—Magnetic resonance imaging.
Otol Neurotol **29:**846–853, 2008.

Vestibular schwannomas (VSs) result from mutations in the tumor suppressor gene *merlin* or *schwannomin* and occur in 2 forms; sporadic, isolated tumors and bilateral tumors occurring in patients with the genetic disease neurofibromatosis Type 2 (NF2) (1–4). Current management of VSs is limited to observation with serial imaging, stereotactic radiosurgery, or radiotherapy, and microsurgical removal (5–8). Although these therapies are generally well tolerated, they occasionally result in deafness, facial paralysis, spinal fluid leak, continued tumor growth, or even malignant transformation (9–14). Vestibular schwannomas arising in patients with NF2 are particularly difficult to manage (15). Most patients develop deafness and other cranial and spinal neuropathies, and many die as a result of their disease (16). The discovery of alternative therapies that limit the growth of schwannomas may be of particular benefit to patients with NF2 (4,15,17).

Understanding the role of the merlin protein in Schwann cell (SC) homeostasis should help guide the development of alternative therapies for patients with schwannomas (3,4). Merlin mediates contact inhibition of cell growth and suppresses the activity of intracellular signaling cascades implicated in tumor formation in many cells, including Ras–mitogen-activated protein kinase/extracellular regulated kinase (ERK) kinase–ERK, phosphatidylinositol-3-kinase/Akt, and c-Jun N-terminal kinase (18–24).

In addition to these intracellular kinases, merlin regulates the subcellular localization and activity of receptor tyrosine kinases (25), including the epidermal growth factor receptor, or ErbB, family of tyrosine kinases (26). Like their SC counterparts, VS cells uniformly express ErbB2 and ErbB3, with a subset also expressing epidermal growth factor receptor or ErbB1 and ErbB4 (27–29). A recent study found increased mRNA expression for ErbB1

Address correspondence and reprint requests to Marlan R. Hansen, M.D., The University of Iowa, 200 Hawkins Dr, 21163 PFP, Iowa City, IA 52242-1078; E-mail: marlan-hansen@uiowa.edu

This was supported by NIH-National Institute of Deafness and other NIDCD KO8 DC006211. Genentech (South San Francisco, CA) provided the trastuzumab used in this study.

and ErbB2 in most VSs, and that ErbB1 expression levels correlate with tumor size (30). In normal SCs, merlin is implicated in the cytoplasmic sequestration of ErbB2 in response to cell-cell contact (26). However, in VS cells, ErbB2 constitutively resides in portions of the cell membrane known as lipid rafts and is active (28,29). This lipid raft localization of ErbB2 in VS cells mirrors the movement of ErbB2 into lipid rafts in proliferating, denervated SCs after axotomy (31). Thus, ErbB receptors represent a potential target for therapies to limit VS growth (27–30,32). Given their involvement in a number of different tumors, several ErbB inhibitors have been developed and are used clinically (33).

Here, we tested the efficacy of 2 ErbB inhibitors on VS growth in a xenograft model of human VSs using nude mice. We report that trastuzumab, a humanized anti-ErbB2 monoclonal antibody, and erlotinib, an inhibitor of ErbB1 and ErbB2 kinase activity (34), both reduce the growth of VS xenografts as measured by magnetic resonance imaging (MRI) during a 3-month interval. Erlotinib, but not trastuzumab, resulted in increased VS cell death in these xenografts. Thus, ErbB inhibitors serve as potential novel therapies for the treatment of schwannomas.

MATERIALS AND METHODS

VS Xenografts

Xenografts were developed in male athymic Ncr Nu/Nu mice (National Cancer Institute, National Institutes of Health, Bethesda, MD, USA) from VS specimens derived from 4 separate patients. All patients provided written, informed consent for use of tumor harvested at time of surgery. The institutional review board at the University of Iowa approved the study protocol, and the University of Iowa Institutional Animal Care and Use Committee approved all animal protocols. Mice were housed in a barrier room and watered and fed rodent chow freely.

Acutely resected VS specimens were transported to the laboratory in ice-cold Hanks balanced salt solution (Invitrogen, Calsbad, CA, USA), cut into approximately 10-mm^3 fragments, and placed into the interscapular fat pad in nude mice anesthetized with ketamine (100 mg/kg; Hospira, Lake Forest, IL, USA) and xylazine (10 mg/kg; Phoenix Scientific, St. Joseph, MO, USA). The grafts were allowed to develop for 4 weeks before initiating any treatment.

Measurement of Tumor Volume

Tumor volume was analyzed by MRI. Mice were removed from the barrier facility and imaged in a small-animal MRI (Varian Unity/INOVA 4.7-T scanner; Varian, Inc., Palo Alto, CA, USA). T2-Weighted images were acquired in the axial and sagittal planes by placing an anesthetized mouse inside a 37.5-mm-diameter transmit/receive volume coil. Slice thickness was 0.5 mm in each plane. To calculate the tumor volume, the surface area of the tumor on each sequential image was analyzed using the measurement tool on Image J software (National Institutes of Health) by drawing a region of interest encompassing the tumor. The reviewer was blinded to the experimental group. The measurements were repeated 3 times in both the axial and sagittal planes, and the average tumor surface area was multiplied by the slice thickness (0.5 mm) to calculate the slice volume. Slice volumes were halved for the initial and final slices of each imaging series. Slice volumes were then summed for total tumor volume. We also calculated total tumor volumes using the entire volume of the initial and final slices for each series. This did not affect the overall results of the experiments. To calculate the relative tumor growth, the initial tumor volume (V_i) was subtracted from the final tumor volume (V_f), and the difference was divided by V_i ($[V_f - V_i] / V_i$) to account for differences in initial xenograft volumes. There was no significant difference in the relative tumor growth rates of the trastuzumab control and erlotinib control animals, and the data from these animals were pooled.

Treatment With ErbB Inhibitors

A total of 19 mice bearing human VS xenografts derived from 4 separate patients were analyzed in this study. The Table 1 presents the distribution of VS specimens used for these studies. In a preliminary experiment, 4 mice were implanted with VSs derived from 2 patients and were randomly divided into 2 groups 4 weeks after tumor implantation. Two mice received trastuzumab (25 mg/kg in 0.25 ml isotonic sodium chloride solution, i.p.; Genentech, South San Francisco, CA, USA) 3 times per week for 2 weeks, whereas 2 animals received saline injections. During the final week of treatment, all mice were injected with bromodeoxyuridine (BrdU; 50 mg/kg, i.p.; Sigma-Aldrich, St. Louis, MO, USA) daily to label dividing cells. After the 2-week treatment interval, the xenografts were harvested and fixed in 4% paraformaldehyde (Sigma-Aldrich).

For the longer-term experiment, the xenografts were derived from 2 additional VSs, and initial MRIs were obtained 4 weeks after tumor implantation. After the initial MRI, the mice were returned to a quarantine room, where they were randomly divided into 3 groups of 5 animals each (15 total). One group received trastuzumab (25 mg/kg, i.p.) 3 times per week. This is similar to trastuzumab doses shown to inhibit growth of xenografts derived from human carcinomas that overexpress ErbB2 (35,36). The second group was gavage-fed erlotinib (50 mg/kg; Genentech) 5 days a week. This is similar to erlotinib doses shown to reduce growth of xenografts derived from non–small cell lung cancer and malignant nerve sheath tumors (37,38). Erlotinib was suspended in a solution of 0.5% methyl cellulose (MP Biomedicals, Solon, OH, USA) and 0.4% Tween-80

TABLE 1. *Number and distribution of vestibular schwannoma samples used in these experiments*

	No. vestibular schwannoma specimens from separate patients from which xenografts were derived	Total number (and distribution) of mice bearing xenografts used in experiment
Experiment 1: Feasibility and cell proliferation.	2	4 (2 control and 2 treated with trastuzumab)
Experiment 2: Tumor growth and cell death.	2	15 (5 control, 5 treated with trastuzumab, and 5 treated with erlotinib)
Total	4	19

(Fischer Scientific, Pittsburgh, PA, USA). The final group of mice served as controls. In this group, 3 animals were gavage-fed erlotinib vehicle, and 2 animals received saline injections for trastuzumab control. Treatment continued for 12 weeks. After completion of the treatment, the mice were once again imaged to analyze final tumor volume, and the xenografts were harvested and fixed in 4% paraformaldehyde.

Immunofluorescence and Terminal Deoxynucleotidyl Transferase–Mediated dUTP-Biotin End Labeling of Fragmented DNA Staining

After fixation, the xenografts were washed in phosphate-buffered saline (PBS) and cryoprotected in 30% sucrose. The samples were then embedded in optimum cutting temperature compound (Thermo Fischer Scientific, Waltham, MA, USA) and cryosectioned at 10 to 15 μm. Frozen sections from the preliminary group of animals were treated with 2N HCl for 30 minutes, permeabilized with 0.8% Triton-X100 in PBS for 20 minutes, and then blocked with blocking buffer (5% goat serum, 2% bovine serum albumin, and 0.8% Triton-X100) for 30 minutes. Next, the samples were incubated in mouse monoclonal anti-BrdU (1:800; Sigma-Aldrich) and rabbit anti-S100 (1:800; Sigma-Aldrich) diluted in blocking buffer for 2 h at 37°C. After several washes in PBS, secondary antibodies (anti-mouse Alexa Fluor 568 and antirabbit Alexa Fluor 488, 1:800 each; Invitrogen) diluted in PBS were applied for 1 hour at room temperature. Nuclei were then labeled with Hoechst 3342 (10 μg/ml; Invitrogen) for 10 minutes, and the slides were mounted and coverslipped. Frozen sections from the longer-term groups of animals were labeled with anti-S100 antibody as previously discussed. After immunostaining, terminal deoxynucleotidyl transferase–mediated dUTP-biotin end labeling of fragmented DNA (TUNEL) was performed as previously described (39), and the nuclei were labeled with Hoechst 3342. Digital images were captured on a Leica DMIRE2 epifluorescence microscope (Bannockburn, IL, USA) equipped with a charge-coupled device camera and Leica FW4000 software.

Determination of Cell Proliferation and Cell Death

Cell proliferation was analyzed by assaying BrdU uptake in xenograft frozen sections as previously described (31). The number of BrdU-positive S100-positive cells was analyzed from digital images from 5 randomly selected ×30 microscopic fields (331 ± 108 VS cell nuclei per ×30 field; mean ± standard deviation [SD]) for each of 3 frozen sections per xenograft (fifteen ×30 microscopic fields per xenograft). The average percentage of BrdU-positive VS cells was analyzed for each xenograft. The investigator was blinded to treatment conditions.

Cell death was analyzed using TUNEL to identify apoptotic VS cells as previously described (39). The number of TUNEL-positive S100-positive nuclei was analyzed from 5 randomly selected ×30 microscopic fields for each of 3 frozen sections per xenograft, and the average percentage of TUNEL-positive cells was analyzed for each xenograft. The investigator was blinded to treatment conditions.

Statistical Analysis

Differences in cell proliferation and cell death were analyzed by Student's 2-tailed *t* test using Excel software (Microsoft, Redmond, WA, USA). Differences in relative tumor growth

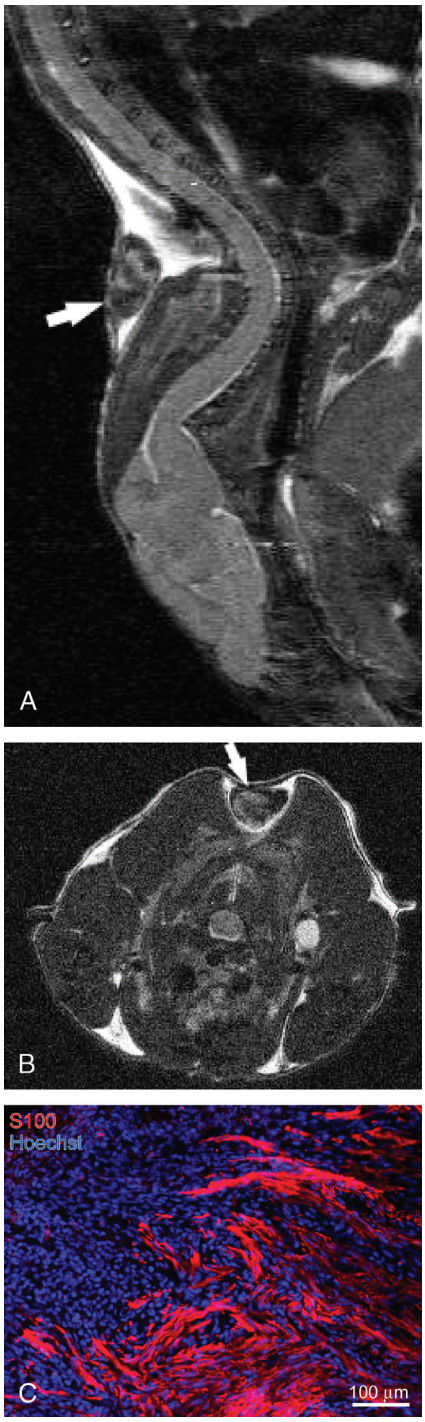

FIG. 1. Human vestibular schwannoma xenograft in nude mice. *A* and *B*, Magnetic resonance imaging of xenografts in sagittal (*A*) and axial (*B*) planes demonstrating survival of xenografts 1 month after implantation. *Arrows* indicate xenografts. *C*, Immunofluorescent labeling of xenograft frozen section with anti-S100 antibody and then Alexa 568 (red) secondary antibody. Nuclei are labeled with Hoechst. This section is taken near the capsule, or edge, of the specimen, demonstrating the S100 labeling of viable tumor cells and the lack of S100 labeling in the capsule cells.

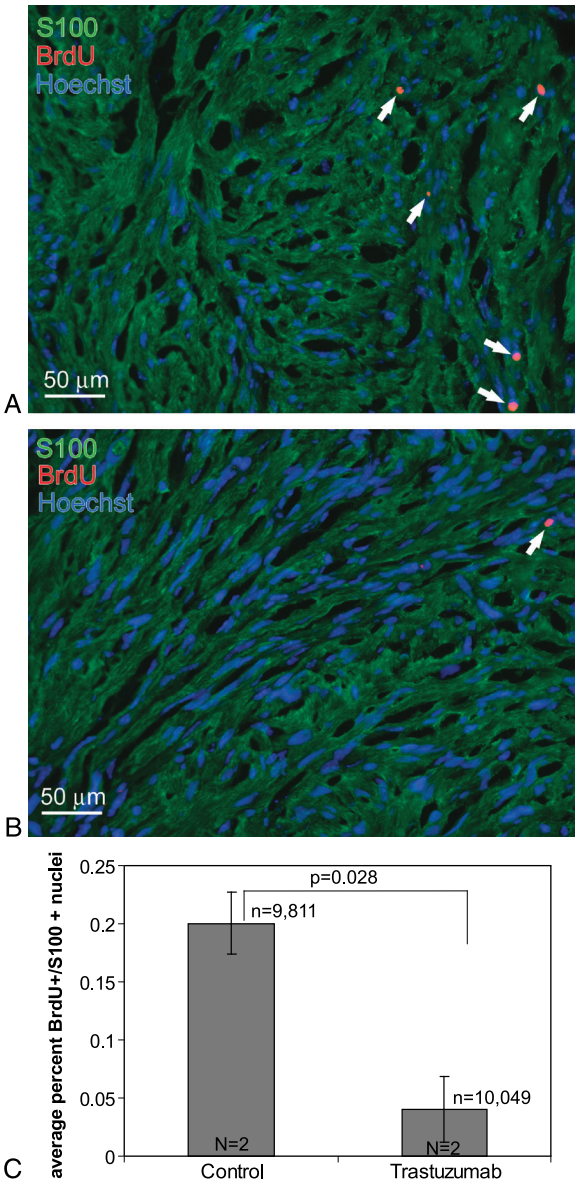

FIG. 2. Trastuzumab inhibits cell proliferation in vestibular schwannoma xenografts. *A* and *B*, Nude mice bearing VS xenografts were treated with saline (*A*; control) or trastuzumab (*B*) for 2 weeks. The animals received daily injections of BrdU to allow identification of proliferating cells. Representative images of xenograft frozen sections immunolabeled with anti-BrdU and anti-S100 antibodies with Alexa 568– (*red*; BrdU-positive) and Alexa 488–conjugated (*green*; S100-positive) secondary antibodies, respectively, are shown. Nuclei were labeled with Hoechst (*blue*). *Arrows* indicate TUNEL-positive nuclei. Scale bar = 50 μm. *C*, The average number of BrdU-positive, S100-positive nuclei was analyzed for each condition from 5 randomly selected fields from 3 to 4 sections per xenograft from 2 separate animals for each group. Trastuzumab significantly reduced BrdU uptake in these xenografts ($p < 0.01$; Student's 2-tailed *t* test). Error bars represent standard error. n indicates total number of VS cells scored for each condition; N, total number of xenografts analyzed for each condition.

were analyzed by 1-way analysis of variance (ANOVA) and then a post-hoc Kruskal-Wallis test using SigmaStat (Systat, Inc., Richmond, CA, USA).

Reagents

Trastuzumab was a generous gift from Genentech. Erlotinib, ketamine, and xylazine were obtained from the University of Iowa Hospitals and Clinics pharmacy. All other reagents were from Sigma-Aldrich unless otherwise specified.

RESULTS

Tumor Imaging and Cell Proliferation

To test the ability of ErbB inhibitors to limit VS growth, we used a xenograft model by transplanting fragments of freshly excised VSs into the interscapular subcutaneous fat of nude mice. Initially, we performed a proof-of-principle experiment to verify that cells in the

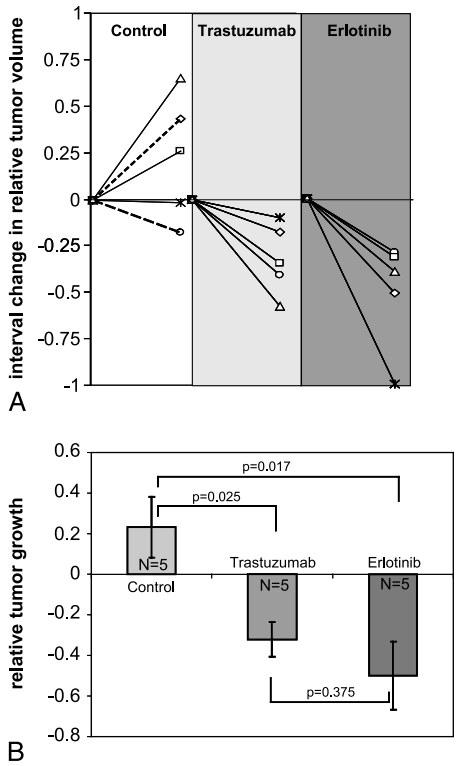

FIG. 3. Trastuzumab and erlotinib reduce the growth of VS xenografts. *A*, The change in relative tumor volume was analyzed by subtracting the initial tumor volume (V_i) from the final tumor volume (V_f) and dividing the difference by the initial tumor volume according to the formula $(V_f - V_i) / V_i$ and is plotted for the 12-week interval for each xenograft. *Dashed lines* in control group represent animals receiving saline, whereas *solid lines* represent animals receiving erlotinib vehicle. *B*, The average relative growth of the xenografts for each condition is plotted. Differences among the means for the treatment groups were analyzed by 1-way ANOVA and then a Kruskal-Wallis test. Error bars represent standard error. Both trastuzumab ($p = 0.025$) and erlotinib ($p = 0.017$) reduced the growth of the VS xenografts compared with controls.

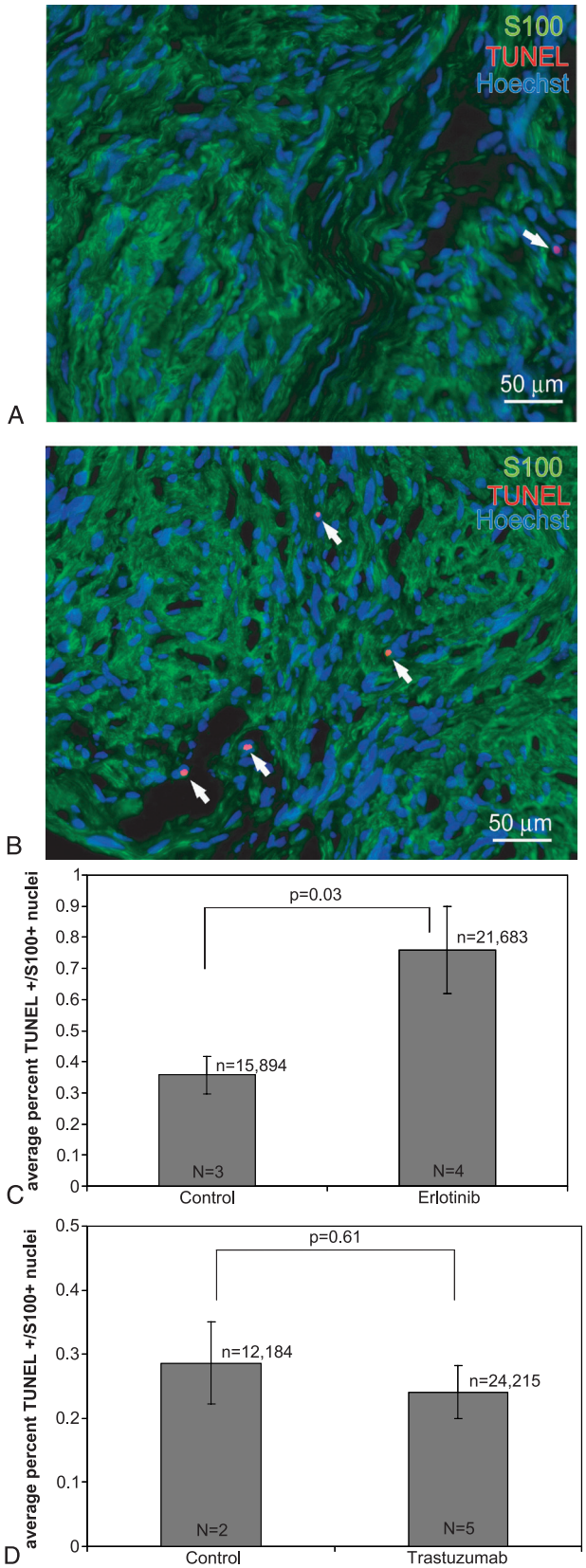

xenografts remained viable and were capable of dividing. We also tested the efficacy of trastuzumab to reduce VS cell proliferation in these xenografts because it has already been shown to reduce VS cell proliferation in vitro (29). Xenografts were allowed to establish for 4 weeks in 4 nude mice. Figure 1 shows representative MRI of xenografts 4 weeks after transplantation. Figure 1 also shows a frozen section immunolabeled with the SC marker anti-S100 antibody and Hoechst (nuclear stain). This section was taken from the edge of the graft to illustrate the specificity of S100 immunolabeling for viable tumor cells compared with the cells comprising the tumor capsule that fail to label with anti-S100 antibody.

After 4 weeks, the animals were randomly assigned to receive trastuzumab (25 mg/kg 3 times a week for 2 wk; 2 animals) or saline injections (2 control animals). All animals were also injected with BrdU daily for the final 7 days before being killed to allow identification of dividing cells. Cell proliferation was analyzed by counting the number of BrdU-positive, S100-positive VS cell nuclei from frozen sections (Fig. 2). The results represent the average percentage of BrdU-positive VS cells for each animal. There was a statistically significant reduction in the percentage of BrdU-positive VS cells in xenografts from trastuzumab-treated animals (0.040 ± 0.029%; mean ± SD) compared with those from control animals (0.201 ± 0.026%; mean ± SD; $p < 0.028$; Student's 2-tailed t test) in the 2-week trial.

Tumor Response to ErbB Inhibitors

Having demonstrated that the xenografts remained viable 4 weeks after implantation and that we can image them with MRI, we performed a second experiment with a separate group of 15 animals to analyze if ErbB inhibition can reduce the growth of the xenografts. Initial MRIs were taken 4 weeks after implantation (Fig. 1). The animals were then randomized to receive trastuzumab, erlotinib, or placebo (the carrier compounds for the pharmaceutical agents) for 12 weeks. After treatment, the animals were reimaged, and the xenografts were harvested to evaluate for cell death. One tumor in the erlotinib-treated group did not appear on the final MRI.

FIG. 4. Erlotinib but not trastuzumab induces cell death in VS xenografts. *A* and *B*, Representative images of xenograft frozen sections from control- (*A*) and erlotinib-treated (*B*) animals immunolabeled with anti-S100 antibody and Alexa 488–conjugated (*green*; S100-positive) secondary antibody. Apoptotic cells were analyzed by TUNEL staining using biotin-labeled dUTP and detected with Alexa 568–labeled streptavidin (*red*; TUNEL-positive). Nuclei were labeled with Hoechst (*blue*). *Arrows* indicate TUNEL-positive nuclei. Scale bar = 50 µm. *C* and *D*, The average number of TUNEL-positive, S100-positive nuclei was analyzed for each condition from 5 randomly selected fields from 3 to 4 sections/xenograft from 3 separate animals for each group. Erlotinib significantly increased the percentage of TUNEL-positive VS cells in these xenografts ($p = 0.03$; Student's 2-tailed t test; *C*) compared with control animals, whereas trastuzumab did not ($p = 0.61$; *D*). Error bars (*C* and *D*) represent standard error. n indicates total number of VS cells scored for each condition; N, total number of xenografts analyzed for each condition.

Relative tumor growth was analyzed by comparing the difference in tumor volumes between the initial and final MRIs normalized to the initial tumor volume. Control animals demonstrated a slight increase in relative tumor volume (0.23 ± 0.15; mean ± standard error [SE]), whereas trastuzumab (−0.32 ± 0.09; mean ± SE) and erlotinib (−0.50 ± 0.16; mean ± SE) resulted in reduction in tumor volume (Fig. 3). The difference in tumor growth was statistically significant between control- and trastuzumab- ($p = 0.025$; 1-way ANOVA and then Kruskal-Wallis) and erlotinib-treated ($p = 0.017$) animals, but was not significantly different between either treatment group ($p = 0.375$).

In Figure 3, control animals (n = 5) receiving saline injections (n = 2) or erlotinib vehicle by gavage (n = 3) were pooled because there was no known biological effect of either placebo, and there was no statistical difference ($p = 0.65$) in relative tumor growth for animals receiving saline (0.13 ± 0.3, mean ± SE) or erlotinib vehicle (0.32 ± 0.28, mean ± SE). If we analyze the data without pooling the control animals, the mean relative tumor growth in animals receiving erlotinib is statistically less than animals receiving erlotinib vehicle ($p = 0.01$; Student's 2-tailed *t* test). Similarly, the mean relative tumor growth in animals receiving trastuzumab trended less than animals receiving saline injections ($p = 0.09$; Student's 2-tailed *t* test).

Erlotinib Induces Cell Death in VS Xenografts

Treatment with ErbB inhibitors caused a reduction in the final tumor volume compared with the initial volume, raising the possibility that the inhibitors may cause death of the VS cells. To examine this possibility, we stained frozen sections of the xenografts with TUNEL that labels apoptotic nuclei. There was no significant difference in the percentage of TUNEL-positive cells between xenografts from animals receiving trastuzumab injections (0.24 ± 0.04%; mean ± SE) compared with saline-injected animals (0.29 ± 0.09%; mean ± SE). However, tumor sections harvested from animals treated with erlotinib demonstrated a significant increase in the percentage of TUNEL-positive cells compared with the placebo controls ($p < 0.01$; Student's 2-tailed *t* test). This control group demonstrated 0.36 ± 0.06% (mean ± SE) TUNEL-positive VS cells compared with 0.76 ± 0.14% (mean ± SE) for the erlotinib-treated group (Fig. 4).

DISCUSSION

In this preliminary study involving a small cohort of animals, we demonstrate that ErbB inhibitors reduce the growth of VS xenografts. These encouraging results need to be replicated with tumors derived from a larger group of patients and in other models of VS disease. Nevertheless, they identify a systemic therapy capable of reducing VS growth in vivo and are particularly relevant to patients with NF2 who often have multiple cranial and spinal neuropathies due to schwannoma growth.

In this study, we did not screen the tumors for *merlin* mutations, and thus, it is not possible to analyze if the effects observed here are mutation specific (40–43). Likewise, the expression of ErbB receptors was not analyzed in these tumors because the entire xenograft specimen was consumed in cell proliferation and death analyses. However, several studies confirm that VSs universally express both ErbB2 and ErbB3, similar to their SC counterparts (27–30,32). Significantly, ErbB2 is activated in VSs and drives cell proliferation (27–29,32). The extent of ErbB1 and ErbB4 expression in VSs is less clear, yet a recent study suggests that ErbB1 expression correlates with tumor size (30).

Models of Vestibular Schwannomas and NF2 Disease

Representative models to evaluate therapeutic agents for VSs and NF2 are lacking. Several investigators have developed VS xenograft models (44–47). In general, these tumors grow very slowly, mimicking their behavior in patients (7,48). Similarly, in our study, control tumors demonstrated slight growth during a 3-month interval. Thus, sophisticated and sensitive imaging modalities are required to detect small differences in tumor growth (44). Here, we used T2-weighted MRI sequences that were able to clearly delineate tumor volumes.

Transgenic animals represent an alternative model of NF2 disease. Heterozygous mice carrying germline mutations in *merlin* ($Nf2^{-}/Nf2^{+}$) develop osteosarcomas and liver tumors but fail to develop schwannomas (49,50). Mice carrying biallelic-targeted deletion of *merlin* exon 2 in SCs develop SC hyperplasia and peripheral nerve schwannomas that can be imaged with MRI, representing a potential model to evaluate therapies aimed at reducing schwannoma formation or growth (51–53). However, these mice do not seem to develop VSs. Cell cultures allow for higher throughput screening and complement animal models. Of particular relevance to the results of these experiments, trastuzumab reduces cell proliferation in primary VS cultures derived from human patients (29).

In addition to tumor imaging, we also analyzed the proliferative capacity of VS cells in these xenografts. Consistent with their slow growth rates, we found that only 0.2% of VS cells incorporated BrdU in control animals treated with daily doses of BrdU for 7 days. By comparison, approximately 0.5% of denervated eighth-nerve SCs in rats incorporate BrdU after 4 systemic doses (Provenzano et al., unpublished data), suggesting that the proliferative rate of VS cells is somewhat comparable to that of denervated SCs. This low proliferative rate is consistent with the slow tumor growth observed on MRI and with the clinical behavior of most VSs in humans.

Potential Therapies for NF2

Understanding the cellular and molecular events contributing to schwannoma formation and growth will help guide the development of novel therapies. Recent studies have identified many of the signaling molecules that are regulated by merlin and are implicated in tumor formation. In particular, several intracellular kinases are inhibited by

merlin, including ERK, Akt, c-Jun N-terminal kinase, and p21-activated kinase (18–24) Because dysregulated activity of these kinases contributes to neoplasia, several inhibitory reagents have been developed and represent potential therapies for VSs (54).

In addition to intracellular kinases, activation of ErbB2, a receptor tyrosine kinase essential for SC development, proliferation, and survival, seems to contribute to SC neoplasia, including VSs (27–29,32,55–58). The contribution of ErbB family members to neoplasia in general is well established, and many molecules that inhibit ErbB family members are used clinically in the management of breast, head and neck, lung, central nervous system, and other malignancies (59). In general, these ErbB inhibitors display fewer side effects than cytotoxic agents and may be more suitable for long-term therapy as would likely be required in NF2 patients (33).

The purpose of this preliminary study was to validate the xenograft model of VS and the general ability of ErbB inhibitors to reduce tumor growth. It was not designed to evaluate the relative efficacy of different ErbB inhibitors, which will require a much larger sample of animals to analyze dose-response relationships. However, the observation that both ErbB inhibitors reduced tumor growth provides encouragement that targeting these molecules may prove effective.

CONCLUSION

In summary, we have shown that trastuzumab and erlotinib reduced the growth of VS xenografts. Although the growth of tumors was very slow, we were able to detect small differences in tumor growth using MRI and complement the imaging studies with assays of cell proliferation and death. These results raise the possibility of using ErbB inhibitors as systemic therapy to limit schwannoma growth in patients with NF2 or those unsuitable for current therapies.

Acknowledgments: The authors thank Dan Thedens for assistance with MRI. Trastuzumab was a generous gift from Genentech.

REFERENCES

1. Rouleau GA, Merel P, Lutchman M, et al. Alteration in a new gene encoding a putative membrane-organizing protein causes neurofibromatosis type 2. *Nature* 1993;363:515–21.
2. Trofatter JA, MacCollin MM, Rutter JL, et al. A novel moesin-, ezrin-, radixin-like gene is a candidate for the neurofibromatosis 2 tumor suppressor. *Cell* 1993;72:791–800.
3. Neff BA, Welling DB, Arkhmametyeva E, et al. The molecular biology of vestibular schwannomas: dissecting the pathogenic process at the molecular level. *Otol Neurotol* 2006;27:197–208.
4. Welling DB, Packer MD, Chang LS. Molecular studies of vestibular schwannomas: a review. *Curr Opin Otolaryngol Head Neck Surg* 2007;15:341–6.
5. National Institutes of Health. National Institutes of Health Consensus Development Conference Statement on Acoustic Neuroma, December 11–13, 1991. The Consensus Development Panel. *Arch Neurol* 1994;51:201–7.
6. Smouha EE, Yoo M, Mohr K, et al. Conservative management of acoustic neuroma: a meta-analysis and proposed treatment algorithm. *Laryngoscope* 2005;115:450–4.
7. Battaglia A, Mastrodimos B, Cueva R. Comparison of growth patterns of acoustic neuromas with and without radiosurgery. *Otol Neurotol* 2006;27:705–12.
8. Wackym PA. Stereotactic radiosurgery, microsurgery, and expectant management of acoustic neuroma: basis for informed consent. *Otolaryngol Clin North Am* 2005;38:653–70.
9. Evans DG, Birch JM, Ramsden RT, et al. Malignant transformation and new primary tumours after therapeutic radiation for benign disease: substantial risks in certain tumour prone syndromes. *J Med Genet* 2006;43:289–94.
10. Bari ME, Forster DM, Kemeny AA, et al. Malignancy in a vestibular schwannoma. Report of a case with central neurofibromatosis, treated by both stereotactic radiosurgery and surgical excision, with a review of the literature. *Br J Neurosurg* 2002;16:284–9.
11. Wilkinson JS, Reid H, Armstrong GR. Malignant transformation of a recurrent vestibular schwannoma. *J Clin Pathol* 2004;57:109–10.
12. Lanman TH, Brackmann DE, Hitselberger WE, et al. Report of 190 consecutive cases of large acoustic tumors (vestibular schwannoma) removed via the translabyrinthine approach. *J Neurosurg* 1999;90:617–23.
13. Meyer TA, Canty PA, Wilkinson EP, et al. Small acoustic neuromas: surgical outcomes versus observation or radiation. *Otol Neurotol* 2006;27:380–92.
14. Slattery WH 3rd, Fisher LM, Iqbal Z, et al. Vestibular schwannoma growth rates in neurofibromatosis type 2 natural history consortium subjects. *Otol Neurotol* 2004;25:811–7.
15. Baser ME, R Evans DG, Gutmann DH. Neurofibromatosis 2. *Curr Opin Neurol* 2003;16:27–33.
16. Otsuka G, Saito K, Nagatani T, et al. Age at symptom onset and long-term survival in patients with neurofibromatosis Type 2. *J Neurosurg* 2003;99:480–3.
17. Hanemann CO, Evans DG. News on the genetics, epidemiology, medical care and translational research of Schwannomas. *J Neurol* 2006;253:1533–41.
18. Lim JY, Kim H, Kim YH, et al. Merlin suppresses the SRE-dependent transcription by inhibiting the activation of Ras-ERK pathway. *Biochem Biophys Res Commun* 2003;302:238–45.
19. Jung JR, Kim H, Jeun SS, et al. The phosphorylation status of merlin is important for regulating the Ras-ERK pathway. *Mol Cells* 2005;20:196–200.
20. Lim JY, Kim H, Jeun SS, et al. Merlin inhibits growth hormone-regulated Raf-ERKs pathways by binding to Grb2 protein. *Biochem Biophys Res Commun* 2006;340:1151–7.
21. Morrison H, Sperka T, Manent J, et al. Merlin/neurofibromatosis type 2 suppresses growth by inhibiting the activation of Ras and Rac. *Cancer Res* 2007;67:520–7.
22. Rong R, Tang X, Gutmann DH, et al. Neurofibromatosis 2 (NF2) tumor suppressor merlin inhibits phosphatidylinositol 3-kinase through binding to PIKE-L. *Proc Natl Acad Sci U S A* 2004;101:18200–5.
23. Chadee DN, Xu D, Hung G, et al. Mixed-lineage kinase 3 regulates B-Raf through maintenance of the B-Raf/Raf-1 complex and inhibition by the NF2 tumor suppressor protein. *Proc Natl Acad Sci U S A* 2006;103:4463–8.
24. Kaempchen K, Mielke K, Utermark T, et al. Upregulation of the Rac1/JNK signaling pathway in primary human schwannoma cells. *Hum Mol Genet* 2003;12:1211–21.
25. Fraenzer JT, Pan H, Minimo L Jr, et al. Overexpression of the NF2 gene inhibits schwannoma cell proliferation through promoting PDGFR degradation. *Int J Oncol* 2003;23:1493–500.
26. Fernandez-Valle C, Tang Y, Ricard J, et al. Paxillin binds schwannomin and regulates its density-dependent localization and effect on cell morphology. *Nat Genet* 2002;31:354–62.
27. Hansen MR, Linthicum FH Jr. Expression of neuregulin and activation of erbB receptors in vestibular schwannomas: possible autocrine loop stimulation. *Otol Neurotol* 2004;25:155–9.
28. Stonecypher MS, Chaudhury AR, Byer SJ, et al. Neuregulin growth factors and their ErbB receptors form a potential signaling network for schwannoma tumorigenesis. *J Neuropathol Exp Neurol* 2006;65:162–75.

29. Hansen MR, Roehm PC, Chatterjee P, et al. Constitutive neuregulin-1/ErbB signaling contributes to human vestibular schwannoma proliferation. *Glia* 2006;53:593–600.
30. Doherty JK, Ongkeko W, Crawley B, et al. ErbB and Nrg: potential molecular targets for vestibular schwannoma pharmacotherapy. *Otol Neurotol* 2008;29:50–7.
31. Brown KD, Hansen MR. Lipid raft localization of erbB2 in vestibular schwannoma and Schwann cells. *Otol Neurotol* 2008;29:79–85.
32. Wickremesekera A, Hovens CM, Kaye AH. Expression of ErbB-1 and 2 in vestibular schwannomas. *J Clin Neurosci* 2007;14: 1199–206.
33. Herbst RS. Review of epidermal growth factor receptor biology. *Int J Radiat Oncol Biol Phys* 2004;59:21–6.
34. Schaefer G, Shao L, Totpal K, et al. Erlotinib directly inhibits HER2 kinase activation and downstream signaling events in intact cells lacking epidermal growth factor receptor expression. *Cancer Res* 2007;67:1228–38.
35. Wang CX, Koay DC, Edwards A, et al. In vitro and in vivo effects of combination of Trastuzumab (Herceptin) and Tamoxifen in breast cancer. *Breast Cancer Res Treat* 2005;92:251–63.
36. Kimura K, Sawada T, Komatsu M, et al. Antitumor effect of trastuzumab for pancreatic cancer with high HER-2 expression and enhancement of effect by combined therapy with gemcitabine. *Clin Cancer Res* 2006;12:4925–32.
37. Friess T, Scheuer W, Hasmann M. Erlotinib antitumor activity in non-small cell lung cancer models is independent of HER1 and HER2 overexpression. *Anticancer Res* 2006;26:3505–12.
38. Mahller YY, Vaikunth SS, Currier MA, et al. Oncolytic HSV and erlotinib inhibit tumor growth and angiogenesis in a novel malignant peripheral nerve sheath tumor xenograft model. *Mol Ther* 2007;15:279–86.
39. Provenzano MJ, Xu N, Ver Meer MR, et al. p75NTR and sortilin increase after facial nerve injury. *Laryngoscope* 2008;118:87–93.
40. Stemmer-Rachamimov AO, Xu L, Gonzalez-Agosti C, et al. Universal absence of merlin, but not other ERM family members, in schwannomas. *Am J Pathol* 1997;151:1649–54.
41. Zucman-Rossi J, Legoix P, Der Sarkissian H, et al. NF2 gene in neurofibromatosis type 2 patients. *Hum Mol Genet* 1998;7:2095–101.
42. Mautner VF, Baser ME, Kluwe L. Phenotypic variability in two families with novel splice-site and frameshift NF2 mutations. *Hum Genet* 1996;98:203–6.
43. Bruder CE, Hirvela C, Tapia-Paez I, et al. High resolution deletion analysis of constitutional DNA from neurofibromatosis type 2 (NF2) patients using microarray-CGH. *Hum Mol Genet* 2001;10: 271–82.
44. Chang LS, Jacob A, Lorenz M, et al. Growth of benign and malignant schwannoma xenografts in severe combined immunodeficiency mice. *Laryngoscope* 2006;116:2018–26.
45. Charabi S, Rygaard J, Klinken L, et al. Subcutaneous growth of human acoustic schwannomas in athymic nude mice. *Acta Otolaryngol* 1994;114:399–405.
46. Lee JK, Kim TS, Chiocca EA, et al. Growth of human schwannomas in the subrenal capsule of the nude mouse. *Neurosurgery* 1990;26:598–605.
47. Lee JK, Sobel RA, Chiocca EA, et al. Growth of human acoustic neuromas, neurofibromas and schwannomas in the subrenal capsule and sciatic nerve of the nude mouse. *J Neurooncol* 1992;14: 101–12.
48. Roehm PC, Gantz BJ. Management of acoustic neuromas in patients 65 years or older. *Otol Neurotol* 2007;28:708–14.
49. McClatchey AI, Saotome I, Mercer K, et al. Mice heterozygous for a mutation at the Nf2 tumor suppressor locus develop a range of highly metastatic tumors. *Genes Dev* 1998;12:1121–33.
50. Gutmann DH, Giovannini M. Mouse models of neurofibromatosis 1 and 2. *Neoplasia* 2002;4:279–90.
51. Giovannini M, Robanus-Maandag E, van der Valk M, et al. Conditional biallelic Nf2 mutation in the mouse promotes manifestations of human neurofibromatosis type 2. *Genes Dev* 2000;14: 1617–30.
52. Messerli SM, Tang Y, Giovannini M, et al. Detection of spontaneous schwannomas by MRI in a transgenic murine model of neurofibromatosis type 2. *Neoplasia* 2002;4:501–9.
53. Messerli SM, Prabhakar S, Tang Y, et al. Treatment of schwannomas with an oncolytic recombinant herpes simplex virus in murine models of neurofibromatosis type 2. *Hum Gene Ther* 2006;17: 20–30.
54. Hirokawa Y, Tikoo A, Huynh J, et al. A clue to the therapy of neurofibromatosis type 2: NF2/merlin is a PAK1 inhibitor. *Cancer J* 2004;10:20–6.
55. Adlkofer K, Lai C. Role of neuregulins in glial cell development. *Glia* 2000;29:104–11.
56. Stonecypher MS, Byer SJ, Grizzle WE, et al. Activation of the neuregulin-1/ErbB signaling pathway promotes the proliferation of neoplastic Schwann cells in human malignant peripheral nerve sheath tumors. *Oncogene* 2005;24:5589–605.
57. Huijbregts RP, Roth KA, Schmidt RE, et al. Hypertrophic neuropathies and malignant peripheral nerve sheath tumors in transgenic mice overexpressing glial growth factor beta3 in myelinating Schwann cells. *J Neurosci* 2003;23:7269–80.
58. Frohnert PW, Stonecypher MS, Carroll SL. Constitutive activation of the neuregulin-1/ErbB receptor signaling pathway is essential for the proliferation of a neoplastic Schwann cell line. *Glia* 2003; 43:104–18.
59. Hsieh AC, Moasser MM. Targeting HER proteins in cancer therapy and the role of the non-target HER3. *Br J Cancer* 2007;97: 453–7.